Proceedings of the Canadian Society for Mechanical Engineering International Congress 2022
CSME Congress 2022
June 5-8, 2022, Edmonton, AB, Canada

A SIMULATION STUDY FOR DISTRIBUTED LOAD MEASUREMENT OF A CYLINDRICAL ROLLING ELEMENT BEARING

Xin Wang[1], Xihui Liang[1*], Nan Wu[1]
[1]Department of Mechanical Engineering, University of Manitoba, Winnipeg, Canada
*xihui.liang@umanitoba.ca

Abstract—In this paper, a relationship between a load applied on the inner ring and strains measured on the outer ring of a bearing is studied. A linear relationship is confirmed under different loading conditions. Finite element analysis of a cylindrical rolling element bearing with 11 rollers is conducted in ANSYS to collect the strain data on the outer ring of the bearing. Static load and varying loads are applied to the inner ring of the bearing. Strains collected on the outer ring show a linear relationship to the radial load applied on the inner ring. The linear coefficient k is identical under static and sinusoid varying loads for each roller. With the linear relationship, a simple method is proposed to calculate the contact force between a roller and the outer ring very accurately with an error of less than 1.5%, according to the simulation results.

Keywords-rolling element bearing; distributed load; strain; linear relationship

I. INTRODUCTION

Rolling bearings are widely used in products and machinery with rotational motion due to their low rolling friction. The primary function of a rolling bearing is straightforward: to bear radial, axial, or combined loads to improve the operation of mechanical transmission systems. Thus, it is essential to comprehensively understand the static and dynamic loads encountered to the rolling bearings to guarantee the system's stability, reliability, and products' durability.

Generally, there are different designs for the rolling bearings with different types of mechanical applications. Thus, interchangeable standards are required to define fatigue or failure measurements and limits. Following these standardized selection criteria, system load information is needed to determine which rolling bearing design is most appropriate for a specific application.

The load distribution on rolling elements is one of the most important operating characteristics of a bearing; this is because it plays an important role in its radial stiffness [1]–[3], static carrying capacity [4], [5], fatigue life [6], [7], vibration and dynamic characteristics [8]–[12]. Many numerical studies and experimental methods have been conducted worldwide for decades. Murer et al. [13] presented a numerical model for measuring the deformation of a bearing ring under a radial load. The deflection was measured using a capacitive probe, and contact force was calculated afterward. They also confirmed the linearity of the load-strain relationship. Their research provided in-site measurements of static loadings applied on a bearing ring and contributed to an early stage of the bearing design. However, they only simulated the distributed loads under a single radial load within the bearing's operational limits. The accuracy and consistency of the results are hard to confirm. In 2020, Kerst et al. [14] proposed a novel approach based on modelling the physical behaviour of the bearing. They introduced a method based on the Kalman filter to study the bearing's strain model and load model. However, they also noticed that the accuracy of the estimated load needed progress due to the relatively larger bulk and local deformation during loading. Ren et al. [15] presented a mathematical model to calculate the radial load distribution on ball and roller bearings. Their research was based on contact deformation and Hertz elastic contact theory. The obtained results were found to be with high accuracy. But their method is only applicable to the static load condition. Hou and Wang [16] proposed an experimental method to determine load distribution by measuring the strain response at the bearing surface with an instrumented housing. The proposed method can measure the static load distribution over rolling elements in the load zone and the real-time dynamic load distribution on specific positions of the load zone. They concluded that the static load distribution matches well with the theoretical calculation. Their dynamic load tests showed a fluctuation around the static load distribution due to the difference among rollers. However, the instrumented housing is complicated and challenging for different applications in their experimental setup.

In order to overcome the load measurement accuracy problem and get rid of the complex measurement set up in the previous studies, the relationship between the strain generated on the outer ring and the load applied on the inner ring is studied. Furthermore, an applicable method is proposed in this research with relatively high accuracy.

II. PROPOSED METHODOLOGY

In this section, the loading condition applied in the research is illustrated first, and then a method to calculate the distributed load on each roller is briefly proposed.

This study is supported by the Natural Science and Engineering Research Council of Canada [Grant No. RGPIN-2019-05361, GRPIN-2021-03356], the University of Manitoba Research Grants Program and the China Scholarship Council (CSC).

As shown in Fig. 1, the inner ring of a bearing is subjected to an external radial load F_r, and it is overlapped with the vertical axis of the bearing and goes towards bottom of the bearing. A series of $F_{n,or}$ would be transmitted to the outer ring through rollers, which are distributed loads. The radial load F_r can be calculated in the form:

$$F_r = \sum_{n=0}^{z-1} F_{n,or} \cos(n\beta) \quad (1)$$

where β represents the angle of two adjacent rollers, $F_{n,or}$ is the transmitted force to the outer ring from the nth roller, and the series of $F_{n,or}$ represent the radial load distribution on a bearing.

In order to determine $F_{n,or}$, the strain $\varepsilon_{n,or}$ generated on the outer wall of the outer ring caused by the transmitted force would be collected in the simulation. The contact between each roller and the inner wall of the outer ring is a straight line; extending it to the outer wall of the outer ring would get a parallel straight line. As shown in Fig. 1, the normal strain $\varepsilon_{n,or}$ is collected in the middle point of the straight line on the outer wall of the outer ring. The relationship between the strain and the distributed load will be studied to calculate the load based on the strain.

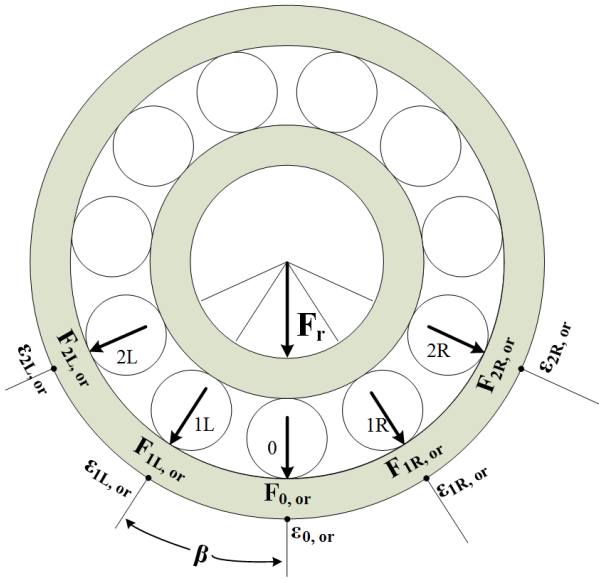

Figure 1. Load distribution on rollers of a cylindrical roller bearing.

III. FEM MODELLING OF A CYLINDRICAL ROLLER BEARING

In this section, the parameters of a rolling bearing are described first, then the modeling is conducted in ANSYS workbench and explained in detail.

A bearing of 11 cylindrical rollers is used in our numerical study (model SKF 305 ECP). Fig. 2 shows the bearing with parameters, and all these parameters are specified in TABLE I.

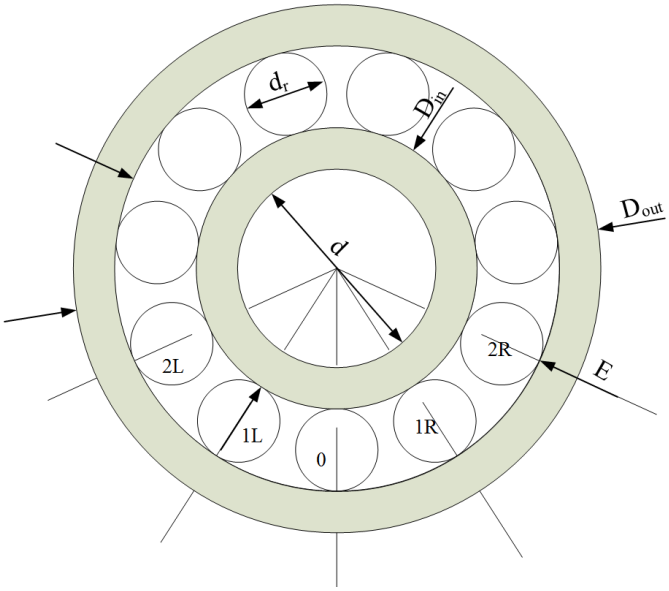

Figure 2. The front view of the cylindrical roller bearing with parameters.

TABLE I. PARAMETERS OF THE CYLINDRICAL ROLLER BEARING

Parameter	Value
Bore diameter (d)	25mm
Outside diameter (D_{out})	62mm
Raceway diameter of the outer ring (E)	54mm
Roller diameter (d_r)	10mm
Width (b)	17mm
Shoulder diameter of the inner ring (D_{in})	34mm
Number of rollers (N)	11
Bearing clearance (C)	0

In order to simulate the force-strain relationship of the bearing, finite element analysis (FEA) was conducted using ANSYS workbench. As shown in figure 3, the force is applied to the inner ring downward during simulation; the upper half of the rollers does not press the outer ring. Therefore, only the contact in the bottom half of the bearing was modelled to reduce the computational cost. The cage was removed to reduce the number of contact surfaces as well. The outer ring is tied to a bearing housing of a cylindrical tube with a thickness of 4 mm.

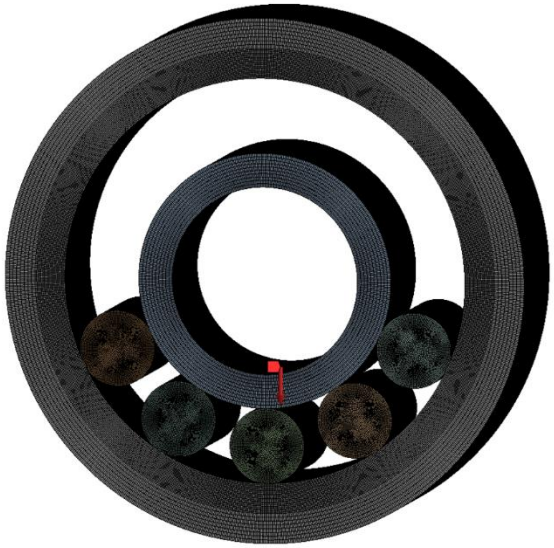

Figure 3. Finite element model of the cylindrical roller bearing with housing.

To prepare for the analysis under the ANSYS workbench, the contact setting between the rollers and inner ring/outer ring is frictional, and the friction coefficient is 0.1. Structural steel material property is assigned to the whole bearing. All the parts are meshed using hexahedral elements. The element size of the outer ring is finer because the strain data would be collected here, which is 0.2 mm. During simulation, the outer surface of the bearing housing is fixed.

IV. FEM Simulation Results and Discussion

Static structural analysis and transient analysis are conducted in the ANSYS workbench to obtain the load-strain results of the rolling element bearing under static load and varying load conditions, respectively. During simulations, the loads are applied to the inner wall of the bearing inner ring in a downward direction. The strain data are collected in five points on the outer wall of the outer ring. They are positioned precisely in the middle of the straight lines on the outer wall of the outer ring parallel to the contact lines between the rollers and the inner wall of the outer ring. In this study, the normal strain generated in the x-direction is recorded. And the relationship between the applied load and the strain generated on the outer ring is discussed specifically under both conditions.

A. *Static structure analysis*

The load applied to the inner ring is constant for the static analysis. Multiple tests are run while the load increases from 500N to 5000N. TABLE II shows the strain data collected in the position on the outer ring ($\varepsilon_{0,\,or}$, $\varepsilon_{1L,\,or}$, $\varepsilon_{1R,\,or}$, $\varepsilon_{2L,or}$, $\varepsilon_{2F,\,or}$ as shown in Fig. 1). And lines drawn based on these data are presented in Fig. 4. Because the rolling element bearing structure is symmetrical, the strain measured in the positions on the left half of the bearing is identical to the strain data on the right half. So, the line of roller 1L is the same as roller 1R; the line of roller 2L is the same as roller 2R. When the deformation of the bearing is small, it still deforms in the elastic range. While the load increases, the strain generated on the roller positions increases. And the relationship between the load and the strain is linear. This linear relationship between the measured strain and the distributed load could be presented by

$$F_{n,or} = k\varepsilon_{n,or} \tag{2}$$

where $F_{n,or}$ is the transmitted force to the outer ring from the nth roller, $\varepsilon_{n,or}$ is the normal strain recorded on the outer ring, and k is a constant indicating the linear relationship between the load and the calculated strain.

TABLE II. THE STRAIN COLLECTED IN THE POSITION ON THE OUTER RING ($\varepsilon_{0,or}, \varepsilon_{1L,or}/\varepsilon_{1R,or}, \varepsilon_{2L,or}/\varepsilon_{2R,or}$)

Load (N)	Strain ($\times 10^{-6}$)		
	$\boldsymbol{\varepsilon_{0,or}}$	$\boldsymbol{\varepsilon_{1L,or}/\varepsilon_{1R,or}}$	$\boldsymbol{\varepsilon_{2L,or}/\varepsilon_{2R,or}}$
500	3.3	2.5	2.4
600	4	3.18	3
700	4.66	3.7	3.52
800	5.33	4.24	4.02
900	6.01	4.77	4.52
1000	6.67	5.33	5.02
2000	13.06	10.7	10.36
3000	19.11	16.3	15.62
4000	25.07	21.95	20.87
5000	30.96	27.63	26.07

Figure 4. The normal strain collected on the outer ring ($\varepsilon_{0,\,or}$, $\varepsilon_{1L,\,or}/\varepsilon_{1R,\,or}$, $\varepsilon_{2L,or}/\varepsilon_{2F,\,or}$).

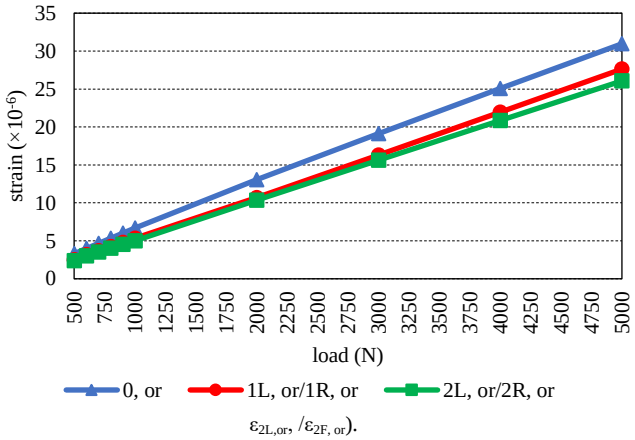

In order to find the constant k, ANSYS simulation with one roller positioned in the bottom ($\varepsilon_{0,\,or}$) is conducted to validate the linear relationship between the radial load and the strain as shown in figure 5. The load is also applied to the inner ring from 1000N to 5000N with an interval of 1000N.

From (2), we have: $F_{0,or} = k\varepsilon_{0,or}$. In the simulation, the load applied to the inner ring is transmitted to the single roller of the simulated bearing. So, $F_r = F_{0,or}$. Hence, $k\varepsilon_{0,or} = F_r$.

The trendline equation displayed in Figure 6 shows that the k calculated in the single roller bearing is 5.06×10^7.

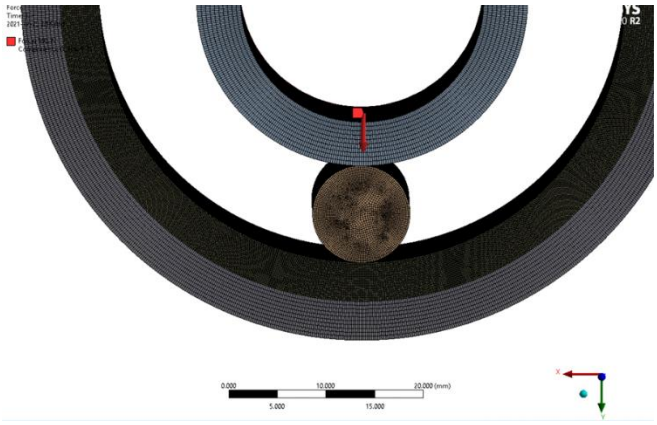

Figure 5. Finite element model of the cylindrical roller bearing with one roller.

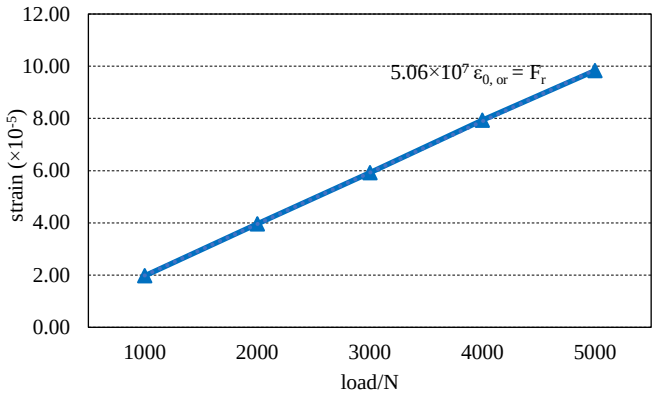

Figure 6. The normal strain collected on the outer ring ($\varepsilon_{0,or}$).

In order to validate the consistency between the results of the one roller bearing and the intact bearing (with 5 strain data collected in the bottom half of the bearing), the distributed load on each roller is calculated by (2), and the results are listed in TABLE III. Meanwhile, the radial load calculated by (1) is also listed in TABLE III as "estimated load."

TABLE III. THE DISTRIBUTED LOAD ON EACH ROLLER ($F_{0,or}, F_{1L,or}, F_{1R,or}, F_{2L,or}, F_{2R,or}$)

Load (N)	Distributed load			Estimated load (N)
	$F_{0,or}$	$F_{1L,or}/F_{1R,or}$	$F_{2L,or}/F_{2R,or}$	
500	167.09	126.58	121.52	481.03
600	202.53	161.01	151.90	599.64
700	235.95	187.34	178.23	699.23
800	269.87	214.68	203.54	800.19
900	304.30	241.52	228.86	900.81
1000	337.72	269.87	254.18	1002.96
2000	661.27	541.77	524.56	2008.62
3000	967.59	825.32	790.89	3013.29
4000	1269.37	1111.39	1056.71	4017.24
5000	1567.59	1398.99	1320.00	5018.10

As shown in the table above, the calculated load is almost identical to the applied radial load with less than 1.5% error.

B. Transient structure analysis

Since the constant k is the same for the single roller bearing model and the intact bearing model with 5 rollers at the bottom under the static load test, we conducted the same test with the single roller bearing model under varying loads to check the k value. Here, the load (F_r) applied to the inner ring varies based on a sinusoid curve, which is $F_r = F_0 + Asin(\omega t)$. In the simulation, the base load F_0 is set to be 500N, and the varying amplitude is 10% of F_0, which is 50N. In order to fulfill the research, we simulated the strain results under varying loads with a low frequency (2π) and a high frequency (100π).

Fig. 7 shows the k results under the sinusoid load, $F_r = 500 + 50sin(2\pi t)$. Fig. 7 (a) shows the applied load to the inner ring varying with time, and the time duration is 1 s. The range of the load is between 450N and 550N. Fig. 7 (b) illustrates the strain collected on the outer ring and the strain changes as the applied load changes. The variation trend is also sinusoid. Fig. 7 (c) calculated the k value, which is the ratio of the strain and the load, and the k value is 5.057×10^7 when the frequency of the load variation is relatively low as 2π. Here, the k value is almost the same as the k value calculated in the static test.

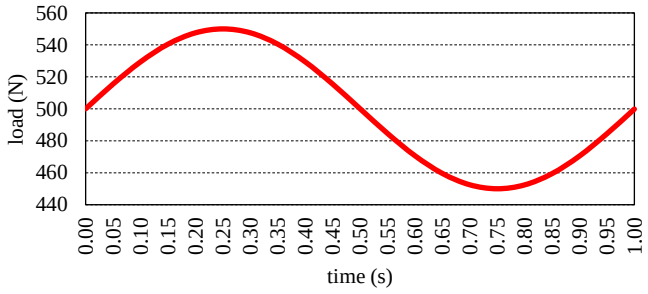

(a)

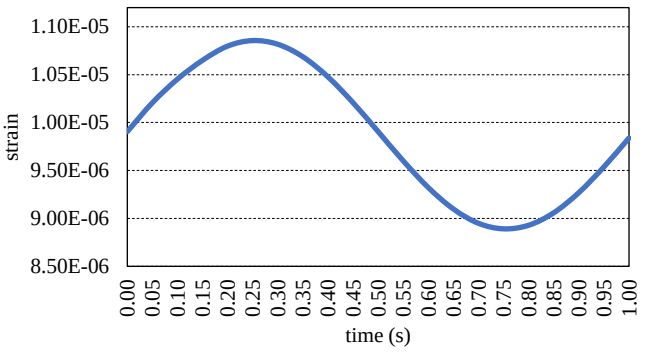

(b)

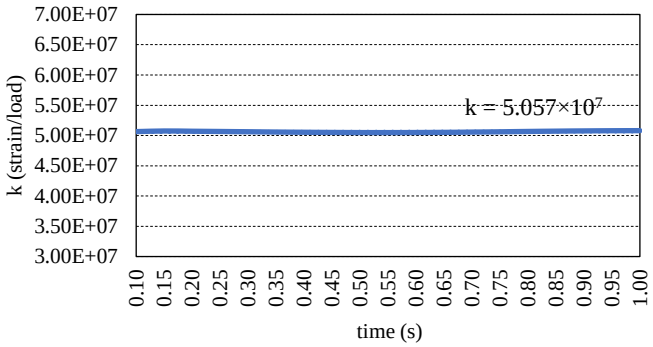

(c)

Figure 7. (a) The radial load applied to the inner ring ($F_r = 500 + 50sin(2\pi t)$). (b) the normal strain collected on the outer ring. (c) the k value, which is calculated by dividing strain by load.

Fig. 8 shows the k results under the sinusoid load, $F_r = 500 + 50sin(100\pi t)$. Here, the load is varying with a relatively high frequency, 100π. Fig. 8 (a) shows the applied load to the inner ring varying with time, and the time duration is 0.01 s. The range of the loads is between 450N and 550N. The strain collected on the outer ring varies with the change of the applied load, and the varying curve is shown in Fig. 8 (b). It is sinusoid as well. The ratio between the strain and the load is calculated to obtain the k value, and the range of the k value is slightly wider compared to the varying load case with lower frequency variation. The K value is around 5.066×10^7 as shown in Fig. 8 (c). When the variation frequency of the applied load is relatively high, the k value is almost the same as the k value calculated in the static test.

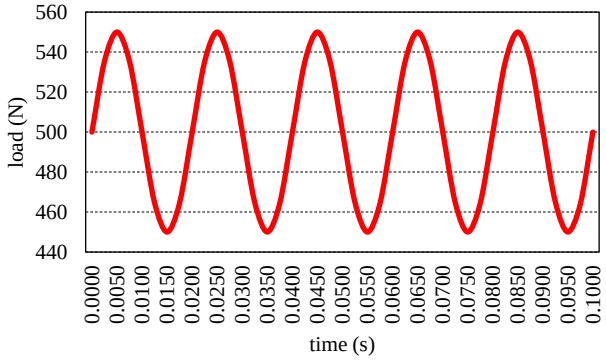

(a)

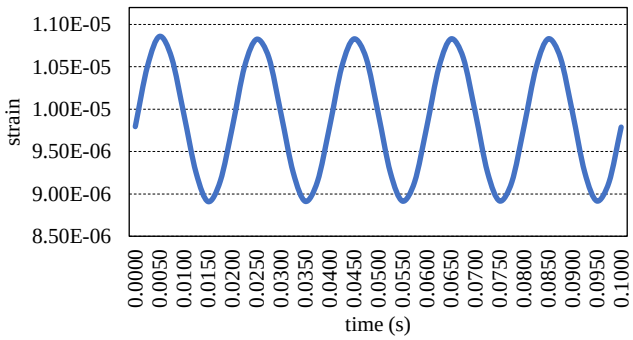

(b)

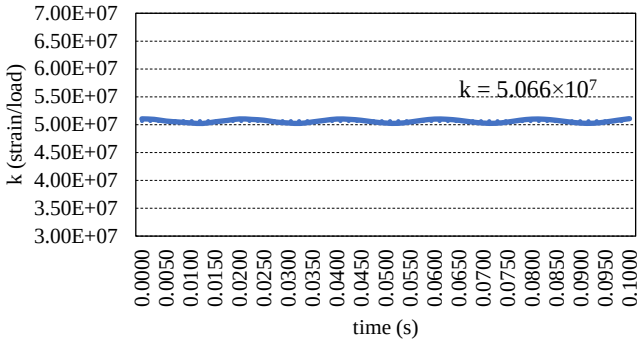

(c)

Figure 8. (a) The radial load applied to the inner ring ($F_r = 500 + 50sin(100\pi t)$). (b) the normal strain collected on the outer ring. (c) the k value, which is calculated by dividing strain by load.

The transient analysis of the intact bearing with 5 rollers in the bottom is conducted to check the linear relationship between the load and the strain and the k value's consistency. Fig. 9 shows the comparison between the "estimated load" calculated by (1) and the applied radial load. Fig. 9 (a) shows the strain varying along time. Fig. 9 (b) illustrates the 5 distributed loads (the distributed loads on the right half are the same as the loads on the left half) calculated by (2), and the k value is set to be 5.06×10^7. Fig. 9 (c) shows the comparison between the sum of the 5 distributed loads calculated by (1) and the applied radial load (F_r). The error of the estimated load compared to the applied load is lower than 1.5%.

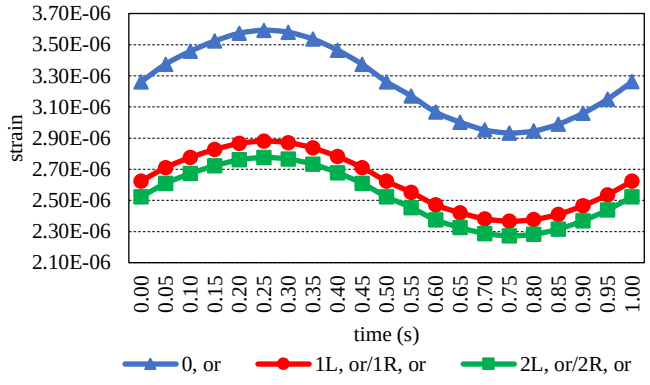

(a)

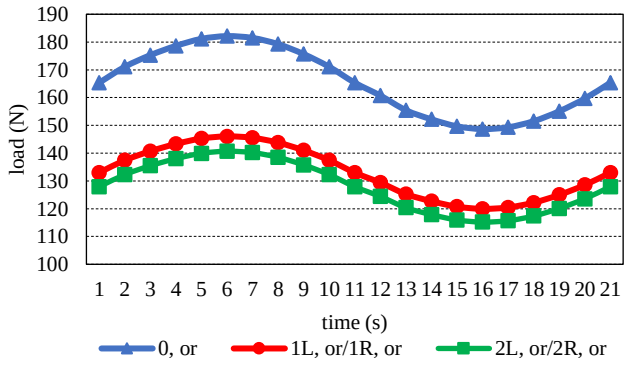

(b)

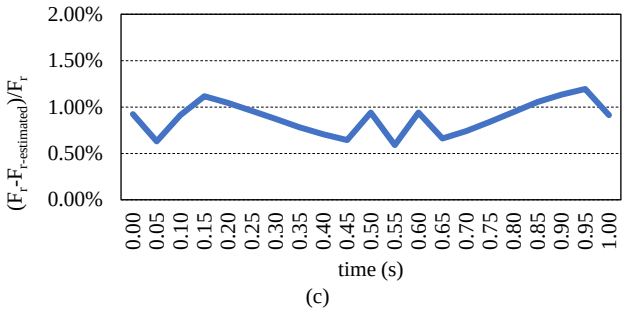

(c)

Figure 9. (a) the x-directional normal strain collected in the outer ring. (b) the distributed load on rollers (k=5.06×10^7). (c) the comparison between the "estimated load" and the applied load.

To sum up, the relationship between the applied load and the strain measured in position on the outer ring in the contact area between the roller and the outer ring is linear, no matter the radial load is static or varying with a sinusoid curve. Thus, it is concluded in the cylindrical roller bearing system that,

$$F_{n,or} = k\varepsilon_{n,or} \tag{2}$$

In the case above, the k value is 5.06×10^7 under static load, varying load with a low variation frequency (2π), and varying load with a high variation frequency (100π).

In order to obtain the k value of the different cylindrical rolling element bearings, the initial static load test could be conducted. By combing (1) and (2), we have,

$$F_r = \sum_{n=0}^{z-1} k\varepsilon_{n,or}\cos(n\beta). \tag{3}$$

Once the strains on the outer ring are measured, the k value could be calculated by (3). Then the distributed load could be calculated by (2).

V. Conclusion

In this research, the linear relationship between the radial load applied on the inner ring of the bearing and the strain collected on the outer ring outside surface is studied and confirmed. The strain data are collected on the outer wall of the outer ring. These points are in the middle of the straight lines on the outer wall of the outer ring parallel to the contact lines between the rollers and the inner wall of the outer ring. In the simulation studies, the linear coefficient k value is calculated under static radial load, sinusoid varying load with a low variation frequency (2π), and sinusoid varying load with a high variation frequency (100π). The k value keeps the same under different loading conditions.

Hence, the initial static load test could be conducted for different cylindrical rolling element bearings to obtain the k value. Then, the distributed load on each roller could be calculated with high accuracy (higher than 98.5%).

References

[1] H. Xu, D. He, H. Ma, K. Yu, X. Zhao, and Y. Yang, "A method for calculating radial time-varying stiffness of flexible cylindrical roller bearings with localized defects," *Engineering Failure Analysis*, vol. 128, p. 105590, Oct. 2021, doi: 10.1016/j.engfailanal.2021.105590.

[2] Y. Han, L. Yang, and T. Xu, "Analysis of static stiffness fluctuation in radially loaded ball and roller bearings," *Arch Appl Mech*, vol. 91, no. 4, pp. 1757–1772, Apr. 2021, doi: 10.1007/s00419-020-01853-6.

[3] D. Petersen, C. Howard, N. Sawalhi, A. Moazen Ahmadi, and S. Singh, "Analysis of bearing stiffness variations, contact forces and vibrations in radially loaded double row rolling element bearings with raceway defects," *Mechanical Systems and Signal Processing*, vol. 50–51, pp. 139–160, Jan. 2015, doi: 10.1016/j.ymssp.2014.04.014.

[4] S. Glodež, R. Potočnik, and J. Flašker, "Computational model for calculation of static capacity and lifetime of large slewing bearing's raceway," *Mechanism and Machine Theory*, vol. 47, pp. 16–30, Jan. 2012, doi: 10.1016/j.mechmachtheory.2011.08.010.

[5] R. Potočnik, P. Göncz, and S. Glodež, "Static capacity of a large double row slewing ball bearing with predefined irregular geometry," *Mechanism and Machine Theory*, vol. 64, pp. 67–79, Jun. 2013, doi: 10.1016/j.mechmachtheory.2013.01.010.

[6] B. Warda and A. Chudzik, "Effect of ring misalignment on the fatigue life of the radial cylindrical roller bearing," *International Journal of Mechanical Sciences*, vol. 111–112, pp. 1–11, Jun. 2016, doi: 10.1016/j.ijmecsci.2016.03.019.

[7] B. Warda and A. Chudzik, "Fatigue life prediction of the radial roller bearing with the correction of roller generators," *International Journal of Mechanical Sciences*, vol. 89, pp. 299–310, Dec. 2014, doi: 10.1016/j.ijmecsci.2014.09.015.

[8] Z. Kıral and H. Karagülle, "Vibration analysis of rolling element bearings with various defects under the action of an unbalanced force," *Mechanical Systems and Signal Processing*, vol. 20, no. 8, pp. 1967–1991, Nov. 2006, doi: 10.1016/j.ymssp.2005.05.001.

[9] B. T. Holm-Hansen and R. X. Gao, "Vibration Analysis of a Sensor-Integrated Ball Bearing," *Journal of Vibration and Acoustics*, vol. 122, no. 4, pp. 384–392, Oct. 2000, doi: 10.1115/1.1285943.

[10] A. Srivani, T. Arunkumar, and S. DenisAshok, "Fourier Harmonic Regression Method for Bearing Condition Monitoring using Vibration Measurements," *Materials Today: Proceedings*, vol. 5, no. 5, pp. 12151–12160, 2018, doi: 10.1016/j.matpr.2018.02.193.

[11] F. Tafinine, "On-line vibration monitoring of bearing faults in induction machine usin Cyclic Spectral Analysis," *MATEC Web Conf.*, vol. 83, p. 09010, 2016, doi: 10.1051/matecconf/20168309010.

[12] W. Li, M. Qiu, Z. Zhu, B. Wu, and G. Zhou, "Bearing fault diagnosis based on spectrum images of vibration signals," *Meas. Sci. Technol.*, vol. 27, no. 3, p. 035005, Mar. 2016, doi: 10.1088/0957-0233/27/3/035005.

[13] S. Murer, F. Bogard, L. Rasolofondraibe, B. Pottier, and P. Marconnet, "Determination of loads transmitted by rolling elements in a roller bearing using capacitive probes: Finite element validation," *Mechanical Systems and Signal Processing*, vol. 54–55, pp. 306–313, Mar. 2015, doi: 10.1016/j.ymssp.2014.07.006.

[14] S. Kerst, B. Shyrokau, and E. Holweg, "A Model-Based Approach for the Estimation of Bearing Forces and Moments Using Outer Ring Deformation," *IEEE Trans. Ind. Electron.*, vol. 67, no. 1, pp. 461–470, Jan. 2020, doi: 10.1109/TIE.2019.2897510.

[15] R. Xiaoli, Z. Jia, and R. Ge, "Calculation of radial load distribution on ball and roller bearings with positive, negative and zero clearance," *International Journal of Mechanical Sciences*, vol. 131–132, pp. 1–7, Oct. 2017, doi: 10.1016/j.ijmecsci.2017.06.042.

[16] Y. Hou and X. Wang, "Measurement of load distribution in a cylindrical roller bearing with an instrumented housing: Finite element validation and experimental study," *Tribology International*, vol. 155, p. 106785, Mar. 2021, doi: 10.1016/j.triboint.2020.106785.